A suspended adsorbent filter for arsenic removal from water to address UN 2030 agenda for sustainable development

Sudipta Pramanik

Independent Researcher (Freelance), Ottawa, ON, K2V 0E4, Canada

Email: sudiptaa.pramanik@gmail.com

TOC Graphic

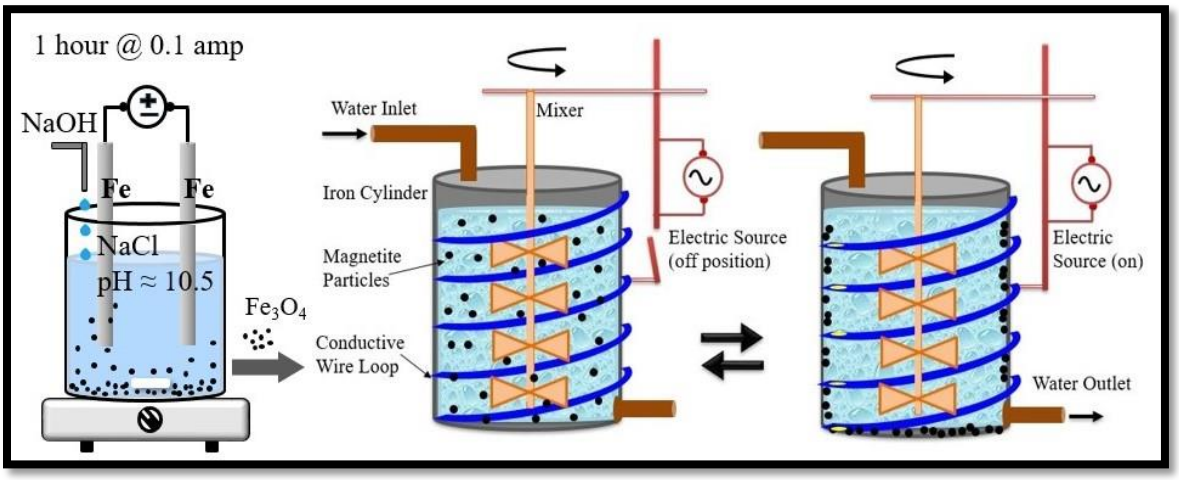

Abstract

Magnetite particles are widely recognized as green and sustainable material for advanced water treatment. The magnetite particles are synthesized through a simple electrochemical process at room temperature from an iron-based electrode immersed in an alkaline aqueous medium at pH 10.5. Arsenic adsorption kinetics were rapid, and adsorption reaction can reach equilibrium within 10 minutes following a pseudo-second-order rate expression with observed reaction rate constants of 0.029 and 0.017 $gmg^{-1}min-1$ for As(III) and As(V), respectively. Magnetite exhibited high adsorption capacity; the equilibrium adsorption capacity of 86.2 and 113.6 mg/gm of magnetite were observed for As(III) and As(V), respectively, at pH 7.0. From Freundlich isotherm, the adsorption intensity parameters for As(III) and As(V) are 0.75 and 0.85, indicating a spontaneous and favorable adsorption of arsenic on magnetite. These results suggest that magnetite can serve as a highly effective adsorbent for fast removal of arsenic and more appealing for decentralized water treatment such as suspended adsorbent filter at the household or community level. The filter

could be a sustainable solution offering environmental remediation to achieve the United Nation's sustainable development goals.

Keywords: arsenic removal, adsorption, magnetite, decentralized water treatment, sustainable development

1. Introduction

Arsenic has been ranked as number one in priority among 20 toxic substances by the Agency for Toxic Substances and Disease Registry (ATSDR) based on its occurrence frequency, toxicity and potential for human exposure (Manning *et al*. 2002; McGavisk *et al*. 2013). Arsenic persists in the environment in several oxidation states. In natural water, arsenic is mostly found in the inorganic form of soluble species as oxyanions of trivalent arsenite, As(III) [H_3AsO_3, $H_2AsO_3^{1-}$, $HAsO_3^{2-}$], and pentavalent arsenate, As(V) [H_3AsO_4, $H_2AsO_4^{1-}$, $HAsO_4^{2-}$]. The pentavalent arsenic species are stable and predominant in the oxygen-rich aerobic environment, whereas the trivalent arsenite species are predominant in a moderately reducing anaerobic environment such as groundwater (Kanel *et al*. 2005, Mohan and Pittman 2007). The inorganic form of arsenic present in natural water is highly toxic in nature. In 1975, the United States Environmental Protection Agency (USEPA) set the drinking water standard for arsenic at 50 µg/L. In 2001, USEPA adopted a lower standard for arsenic contamination in drinking water, considering the effects of long-term and chronic exposure to arsenic. The revised maximum contaminant level (MCL) of arsenic in drinking water is 10µg/L (Foster *et al*. 2019).

Over 200 million people worldwide are at risk of arsenic poisoning from drinking water contamination. Countries in the south and southeast of Asia, such as, Bangladesh, India, China, Nepal, and Pakistan are extremely affected by arsenic contamination in groundwater. In terms of population exposed, arsenic contamination in the groundwater of Bangladesh and India (West

Bengal) represents the most serious calamity identified globally; over 50 million people are suffering from groundwater arsenic contamination in the Ganga basin (Smith *et al*. 2000; Nicomel *et al*. 2016; Chakraborti *et al*. 2018; Shaji *et al*. 2021; Bundschuh *et al*. 2022). According to the United Nation's World Water Report, the global water quality is degraded with the declining of groundwater levels and around 66% of the global extracted groundwater is concentrated on the severity of arsenic poisoning in South and Southeast Asia (Marghade *et al*. 2023).

The 2030 Agenda for sustainable development is an ambitious set of global goals and targets which has been adopted by the United Nations General Assembly in September 2015. Groundwater is a key resource for the achievement of the UN Sustainable Development Agenda for 2030. Arsenic is considered as one of the priority chemical contaminants globally because of its extensive presence in groundwater. The United Nation's sustainable Development Goals (SDGs) cannot be achieved without monitoring and remediating arsenic pollution in groundwater along with microbial water quality. More than 50 SDG indicators, across more than 12 goals, have been identified which are directly or indirectly linked to arsenic and arsenicosis crisis. More than 500 million people in low- and middle-income countries impacted by arsenic contamination in groundwater is a barrier to achieving these goals. To achieve the SDGs targets by the stipulated deadline of 2030, there is an immediate need to mitigate arsenic contamination. Thus, it is necessary to come up with a viable arsenic removal technology to manage the dependency on groundwater effectively (Johnston 2016; Nicomel *et al.* 2016; Shaji *et al*. 2021; Bundschuh *et al*. 2022; Yadav *et al*. 2022; Sarkar *et al*. 2023).

There are various methods to remove arsenic from water which are typically a combination of chemical and physical processes. The commonly used technologies include chemical precipitation, adsorption, ion exchange, reverse osmosis, electrocoagulation, and membrane separation. These

arsenic removal technologies can be effective while there are some drawbacks associated with each of the processes. Adsorption and chemical precipitation techniques are being investigated most to develop an effective and low-cost treatment process. Adsorption is considered as one of the most promising treatment technologies for arsenic removal as it offers several advantages like, high removal efficiency, easy operation and handling, and cost-effectiveness. Intensive studies have been carried out to develop various adsorbents for arsenic removal from water. Various strategic methods have been used to improve the sorption capacity of adsorbents which could complicate the synthesis process and consequently increase the production costs. There is demand for ideal adsorbents to remove arsenic from water in a more efficient way (Clifford *et al*. 1999; Hering *et al.* 1997; Wang *et al*. 2015; Nicomel *et al*. 2016; Qasem *et al*. 2021; Shaji *et al*. 2021; Yadav *et al*. 2022).

Iron-based adsorbents established an effective treatment technology for arsenic removal because of their strong affinity for arsenic species under natural pH conditions. Iron-based adsorbents have higher arsenic removal efficiency at lower cost relative to other adsorbents. Iron compounds, particularly iron oxides, have exhibited arsenic removal in an effective way due to their super-paramagnetic properties. The super-paramagnetic property allows for high arsenic adsorption capacity and efficient separation of adsorbents from water simultaneously. Magnetite, the most magnetic of all the naturally occurring minerals, has emerged as a viable alternative due to its high adsorption capacity, unique super-paramagnetic property, non-toxicity, high efficiency separation and capture by low magnetic fields, and similar affinity for both As (III) and As (V) species. Magnetite is widely recognized as a green and sustainable material for advanced water treatment, offering a cost-effective solution for environmental remediation (Feng *et al*. 2012; Farrell *et al*. 2014; Nikic *et al*. 2019; Jain R. 2022).

The goal of this study was to investigate the application of laboratory-synthesized iron-based adsorbents for the removal of arsenic from aqueous solutions. The main objectives of this article include (i) synthesis and characterization of the adsorbent, (ii) determining the arsenic adsorption capacity of the adsorbent, (iii) investigating factors that affect arsenic (III) adsorption, (iv) compare arsenic (III) removal efficiency of the adsorbent with other adsorbent and conduct preliminary assessment about adsorbent's capacity to remove arsenic from real-life groundwater samples, and (v) configure a suspended adsorbent filter for arsenic removal from water.

The study was conducted at the Indian Institute of Technology, Bombay, during the years 2003 to 2004, as the author's research project for master's program excluding objective (v), i.e. suspended adsorbent filter configuration for arsenic removal from water.

2. Materials and Methods

2.1. Materials

The chemicals used in the experiments were analytical reagent grade and used without any further purification. All glassware used in the experiments was thoroughly cleaned with an acid cleaning solution (sulfuric acid based chromic acid solution) and then rinsed with distilled water. The standard for arsenic (III) stock solution was prepared by dissolving 1.32 gm of primary standard grade arsenic trioxide (As_2O_3) (S.D. Fine Chem Ltd, India) in distilled water containing 1% (w/w) sodium hydroxide (NaOH) and then diluted with distilled water to make one liter of solution. Arsenic (V) stock solution was prepared by dissolving 0.416 gm of sodium arsenate (Na_2HAsO_4, $7H_2O$) (Loba Chemie, India) salt in distilled water to make one liter of solution. The intermediate and secondary standards of arsenic solutions were prepared freshly for each experiment from arsenic stock solutions. The working arsenic solutions used in the experiments were a mixture of appropriate amounts of arsenic stock solutions and tap water. The pH of the tap water varied from

7.2 to 7.5 and there was no detectable amount of arsenic present in tap water. The desired pH of the working arsenic solutions was adjusted by adding either diluted HCl or NaOH.

2.2. Synthesis of adsorbent

The iron oxide-based adsorbent was synthesized in the laboratory by a simple electrochemical method. Initially, it was hypothesized that the electrochemical process would generate Ferrate (VI); a six-valence oxidation states of iron having strong oxidizing ability. The electrochemical synthesis of the adsorbent was conducted in a 1.5 liter glass beaker with two iron electrodes of similar dimensions at room temperature. Before using, the electrodes were rubbed with sandpaper to remove the scale and then rinsed with 1N H_2SO_4 and distilled water, successively. Aqueous sodium chloride solution was used as an electrolyte by dissolving 4.0 gm of sodium chloride in 1 litre of distilled water and the pH of the solution was stabilized at 10.5 by dropwise addition of 1N NaOH. A direct current density of 0.1 ampere was applied to the terminal electrodes by a stabilized power supply for 1 hour and magnetic stirrer was used for uniform mixing during the synthesis process. The supernatant was decanted, and the settled deposit was washed with distilled water and then air dried at room temperature for its subsequent characterization. The identity of the electrochemically synthesized iron oxide-based adsorbent was confirmed as magnetite by X-ray diffraction (XRD) and Fourier transform infrared spectroscopy (FTIR).

2.3. Arsenic Adsorption Kinetics

The kinetics study was performed using an initial concentration of 1.0 mg/L As (III) and As (V) at pH 7.0. The adsorption kinetics were evaluated varying time from 10 to 180 minutes at room temperature. Magnetite (14 mg/L) was continuously mixed with arsenic solutions and samples of the supernatant were withdrawn at 10, 15, 20, 30, 40, 50, 60,120, and 180 minutes. Samples were

immediately centrifuged at 3500 rpm and analyzed for residual arsenic concentration. The rate constants were calculated using the conventional rate expression.

2.4. Arsenic Adsorption Isotherm

Arsenic adsorption isotherm experiments were conducted at a pH of 7.0 with initial arsenic (III) and arsenic (V) concentrations ranging from 10 to 2500 µg /L. The adsorption experiments were carried out in 200 mL plastic bottles containing 14 mg/L of magnetite suspended in 100 mL of arsenic (III) or arsenic (V) solutions with varying arsenic concentrations. A rotary shaker was used to ensure consistent mixing of magnetite with arsenic solutions at room temperature for 1 hour at a speed of 30-35 rpm. After shaking, the bottles were allowed to stand for 10 minutes for solid liquid separation and then the mixtures were centrifuged at 3500 rpm for 2 minutes. The supernatant solutions were analyzed for residual arsenic (III) and arsenic (V) concentration using a spectrophotometer.

2.5. Factors Affecting As (III) Adsorption

Experiments were carried out to investigate the effect of operational factors such as pH, adsorbent dose, and initial arsenic concentrations on As (III) removal by magnetite. To evaluate the effects of pH, isotherm experiments were conducted at initial arsenic (III) concentrations varied from 100 to 1000 µg/L with magnetite dose of 14 mg/L. Solution pH values were adjusted at 6, 7, and 8 by adding dilute HCl and/or NaOH. The effect of adsorbent dose was determined from arsenic (III) adsorption experiments with varying magnetite doses at pH 7.0. Magnetite dose was varied between 4 and 24 mg/L at an initial arsenic (III) concentration of 2 mg/L. The effect of initial arsenic concentration was evaluated from arsenic (III) removal efficiency of 14 mg/L magnetite with varying initial arsenic concentration at pH of 7.0.

2.6. Comparison of arsenic removal efficiency of magnetite with activated alumina and its arsenic removal capacity from real-life groundwater

Arsenic (III) adsorption experiments were conducted with magnetite and activated alumina to compare their arsenic adsorption capacities at pH 7.0. The efficiency of synthesized magnetite to remove arsenic from a real-life groundwater sample was tested in a bench-scale study. Natural groundwater sample used in this study was collected from arsenic-contaminated area of Malda, one of the most severely arsenic affected districts of West Bengal, India. The groundwater sample was acidified and stored in a plastic bottle upon collection in the field for laboratory study. An adsorption isotherm experiment was conducted to examine the efficiency of magnetite in real-life applications to remove arsenic from water.

2.7. Analytical Method

Arsenic concentration in an aqueous sample was determined using the molybdenum blue method (Johnson and Pilson 1972). Arsenic was analyzed by an atomic absorption spectrophotometer. Spectrophotometric measurements were made at a wavelength of 865 nm using absorbance cells of 40 mm path length for arsenic analysis. A calibration curve for total arsenic was prepared from standards in the range of 10 to 1000 μg/L and blanks were run along with samples.

3. Results and Discussion

3.1. Characterization of Magnetite

The X-ray Diffractometer (XRD) and Fourier transform infrared spectrometer (FTIR) were employed to detect the crystalline structure and primary functional groups of the iron-oxide-based adsorbent. The characterization process has identified the adsorbent as magnetite. An X-ray diffraction (XRD) scan was carried out at the Department of Metallurgical Engineering and Materials Science at the Indian Institute of Technology, Bobay, India. The X-ray diffraction

pattern of magnetite shown in *Figure 1* reveals six strong diffraction peaks at 30.5°, 35.9°, 43.5°, 57.5°, and 63°, corresponding to (220), (311), (400), (511), and (440) crystalline planes of magnetite phase, respectively. The less intense peak at 54° (422) is overlapped by the noise and disappeared. The magnetite sample was air-dried at room temperature before XRD characterization. Air drying can cause agglomeration in magnetite particles and in turn create noise in XRD data. The X-ray diffraction pattern of the sample matches well with the standard XRD pattern of magnetite (Cheng *et al*. 2010; Fajaroh *et al*. 2012).

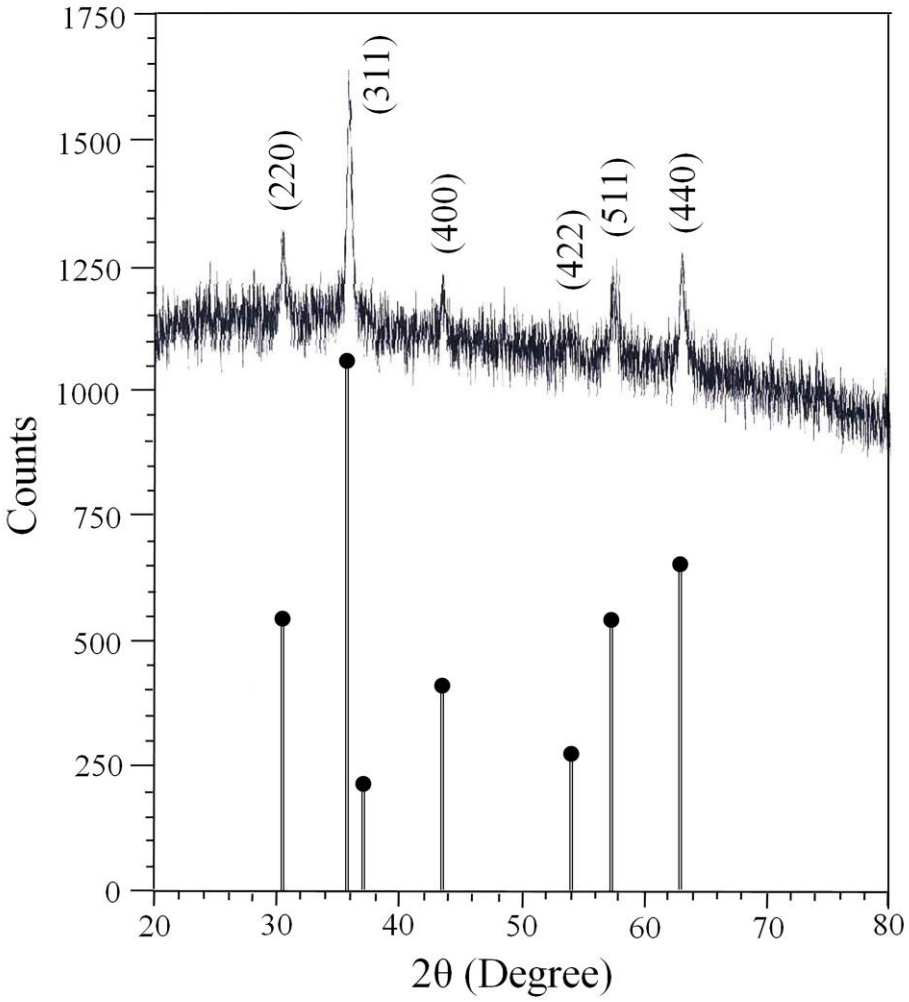

Figure 1: The X-ray diffraction pattern of magnetite sample

The FTIR spectrum of the sample shown in *Figure 2* validates that the sample is magnetite. The absorption band in a region with a high wavenumber is due to the stretching of OH, and in a region with a lower wavenumber, it is a result of the vibration of the Fe–O lattice. The presence of FTIR peaks near 591 cm^{-1} and 450 cm^{-1} is a confirmation of magnetite (Fe_3O_4) formation, as they are associated with metal oxygen (Fe-O) stretching modes in the tetrahedral and octahedral sites, respectively (Zhang *et al*. 2010; Cabrera *et al*. 2008; Fajaroh *et al*. 2012). Existence of water molecules was observed in the FTIR spectrum as the sample was only air-dried at room temperature. Adsorbed water in the magnetite sample features the major band at 3130 cm^{-1} that correspond to the O-H stretching mode of vibration from the water in the sample. The peak at 1624 cm^{-1} in the FTIR spectrum typically corresponds to the bending vibrations of the O-H group in water molecules or hydroxyl groups attached to the surface of the magnetite's crystalline lattice. Peaks around 1400 cm^{-1} can be associated with O-H bending vibrations of water molecules or surface hydroxyl groups on the iron oxide particles. The presence of NaOH as a synthesis agent is consistent with the formation of iron hydroxide or oxyhydroxide intermediates, which can have these hydroxyl groups. A peak around 1031 cm^{-1} in a hydrated iron oxide spectrum often results from Fe-O-H bending vibrations within the iron oxide's structure (Cabrera *et al*. 2008; Chaki *et al*. 2015).

The electrochemically synthesized magnetite is black and attracted to a common magnet. The magnetite particles have a specific surface area of 51.76 m^2/g. The magnetite sample was dried at 105^0C for 1 hour prior to surface area determination by a surface area analyzer.

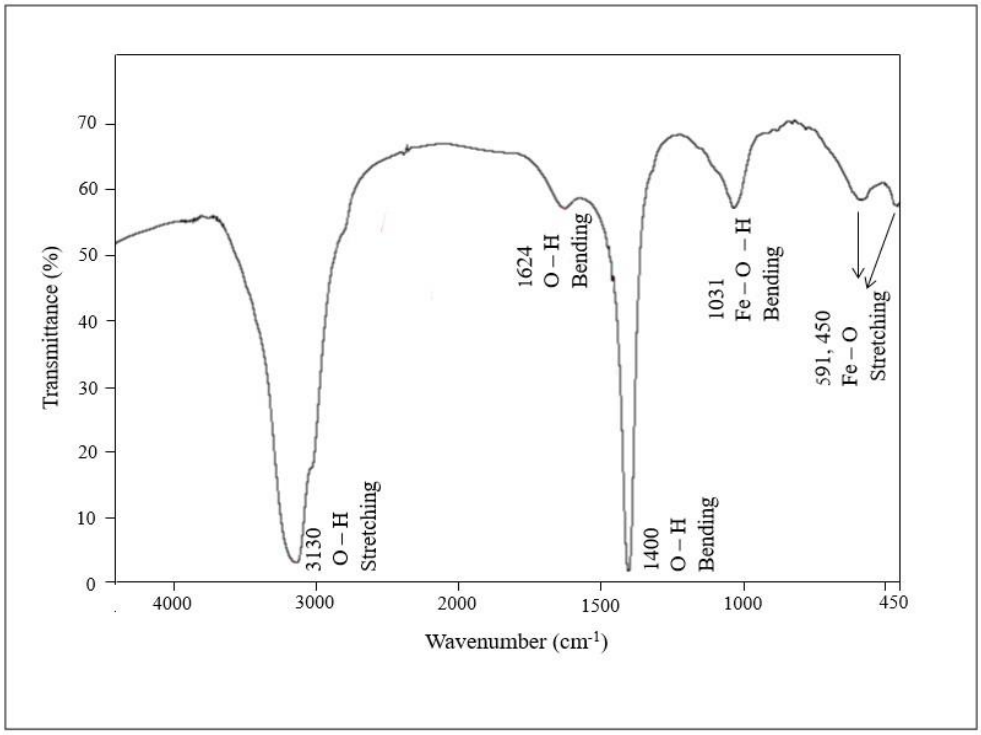

Figure 2: The FTIR spectrum of the magnetite sample

3.2. Formation Mechanism of Magnetite

During the electrochemical synthesis process, a rapid change in the color of the electrolyte was observed. The colorless electrolyte solution turned to brown-red during the first minutes of the reaction process and finally changed to black. In the electrolysis process, the OH^- ion was generated at the cathode and the iron anode is oxidized into a ferric ion. In the electrolyte solution, the formation of ferric hydroxide is favored under alkaline conditions (pH 10.5) and apparently leads to the efficient production of magnetite. The following chemical reactions were presumed to take place during the electrochemical process (Cabrera *et al*. 2008; Franger *et al*. 2004; Starowicz *et al*. 2011; Reséndiz-Ramírez *et al*. 2022).

Cathode: $H_2O + e^- \longrightarrow ½\ H_2 + OH^-$

Anode: $Fe \longrightarrow Fe^{3+} + 3e^-$

Solution: $Fe^{3+} + 3OH^- \longrightarrow Fe(OH)_3$

$$3Fe(OH)_3 + \tfrac{1}{2} H_2 \longrightarrow Fe_3O_4 \downarrow + 5H_2O$$

3.3. Arsenic Adsorption Kinetics

The kinetics of As (III) and As (V) adsorption on magnetite were investigated to determine the arsenic adsorption rate and equilibrium time. The experimental results showed that the adsorption reaction was fast, and equilibrium was achieved within the first few minutes for both arsenite and arsenate. The arsenic adsorption kinetics at pH 7.0 are shown in *Figure 3*, indicating that both arsenic (III) and (V) have similar adsorption patterns and most of the adsorption reactions reach equilibrium within 10 minutes. The parameters of the pseudo-second-order model and coefficient of determination (R^2) are summarized in *Table 1*. The equilibrium adsorption capacity (Q_e) of As (V) was higher than As (III) at pH 7.0, whereas the rate constant for As (III) is slightly higher compared to As (V) indicating faster equilibrium attainment. The solution pH was an important factor affecting the adsorption performance as the pH value significantly affects the rate of the adsorption reaction by influencing the surface charge of the magnetite particles. As (V) adsorption on magnetite is typically favored by acidic conditions due to electrostatic attraction with the positively charged surface, whereas As (III) adsorption is maximum at neutral pH (Jain R. 2022; Wang *et al*. 2022). The high R^2 values indicate that the pseudo-second-order model was suitable to describe the As (III) and As (V) adsorption kinetics on magnetite, and the process was controlled by chemisorption (Ho and McKay 1999).

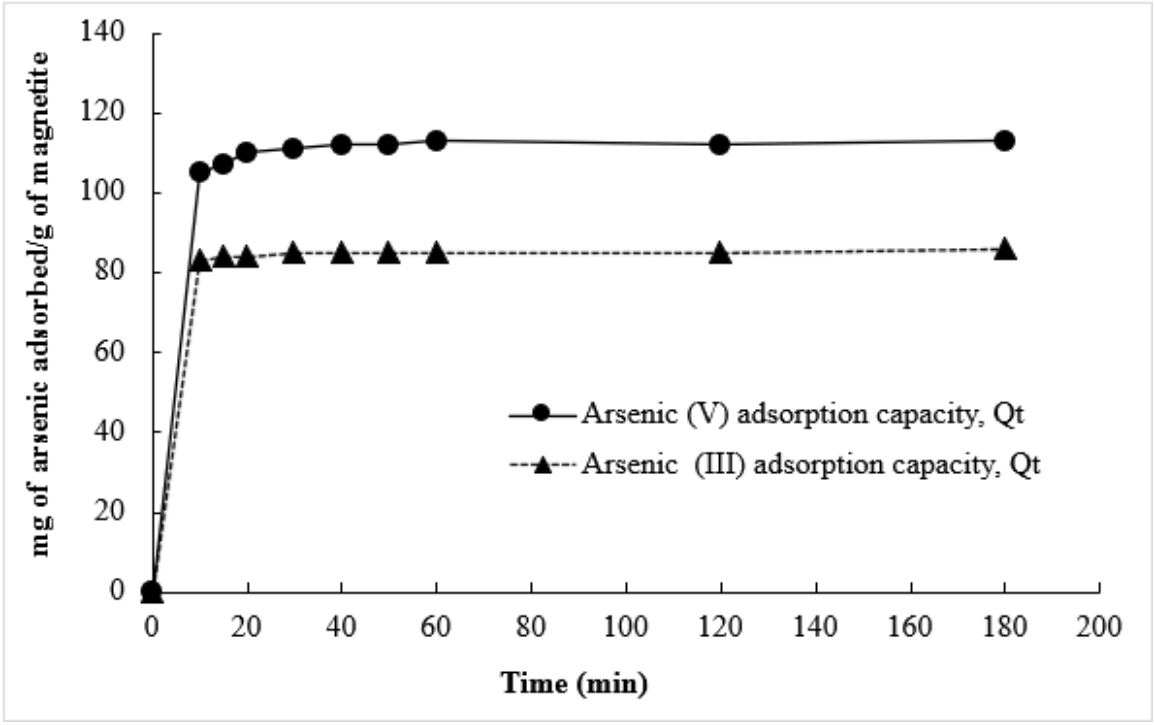

(a)

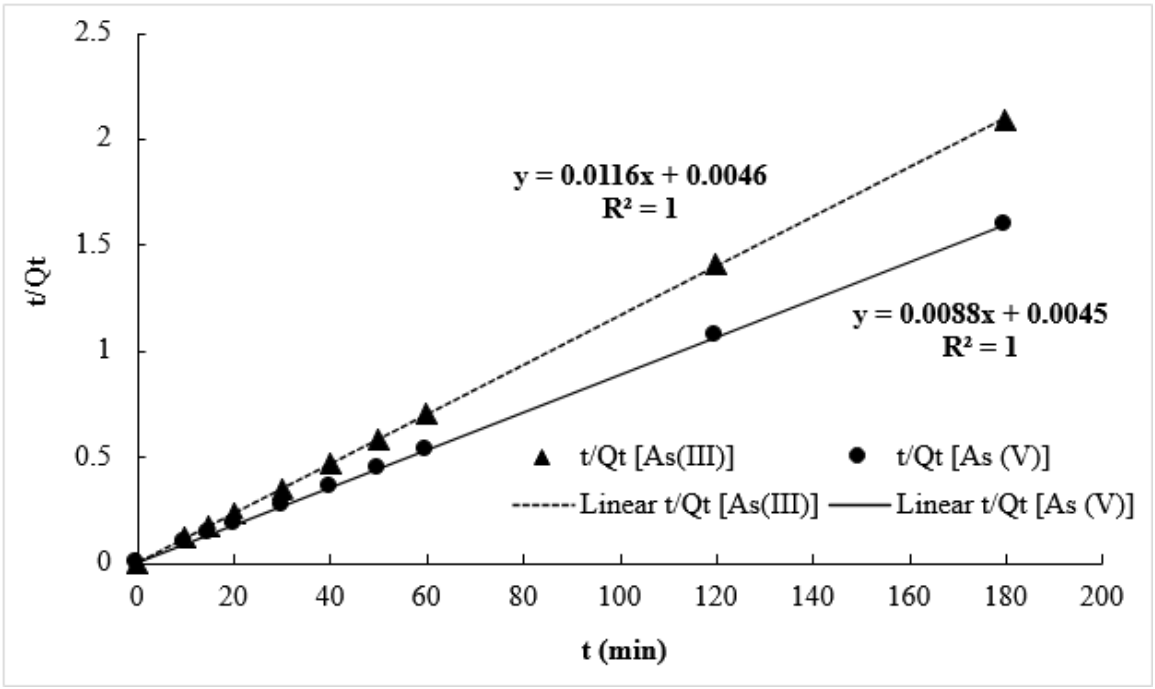

(b)

Figure 3: (a) Adsorption kinetics of arsenic on magnetite at pH 7.0 **(b)** Adsorption kinetics of arsenic fitted with pseudo-second-order model

Table 1: Parameters of pseudo-second-order kinetics for arsenic adsorption on magnetite

Arsenic species	Equilibrium adsorption capacity Q_e (mg g^{-1})	Rate constant k_2 (g $mg^{-1}min^{-1}$)	R^2
As (III)	86.2	0.029	1.0
As (V)	113.6	0.017	1.0

3.4. Arsenic Adsorption Isotherms

The distribution of the arsenic species on the surface of magnetite particles at equilibrium conditions can be explained by adsorption isotherm. The results are presented in terms of equilibrium arsenic concentrations against arsenic adsorption capacities of magnetite at pH 7.0, shown in *Figure 4*.

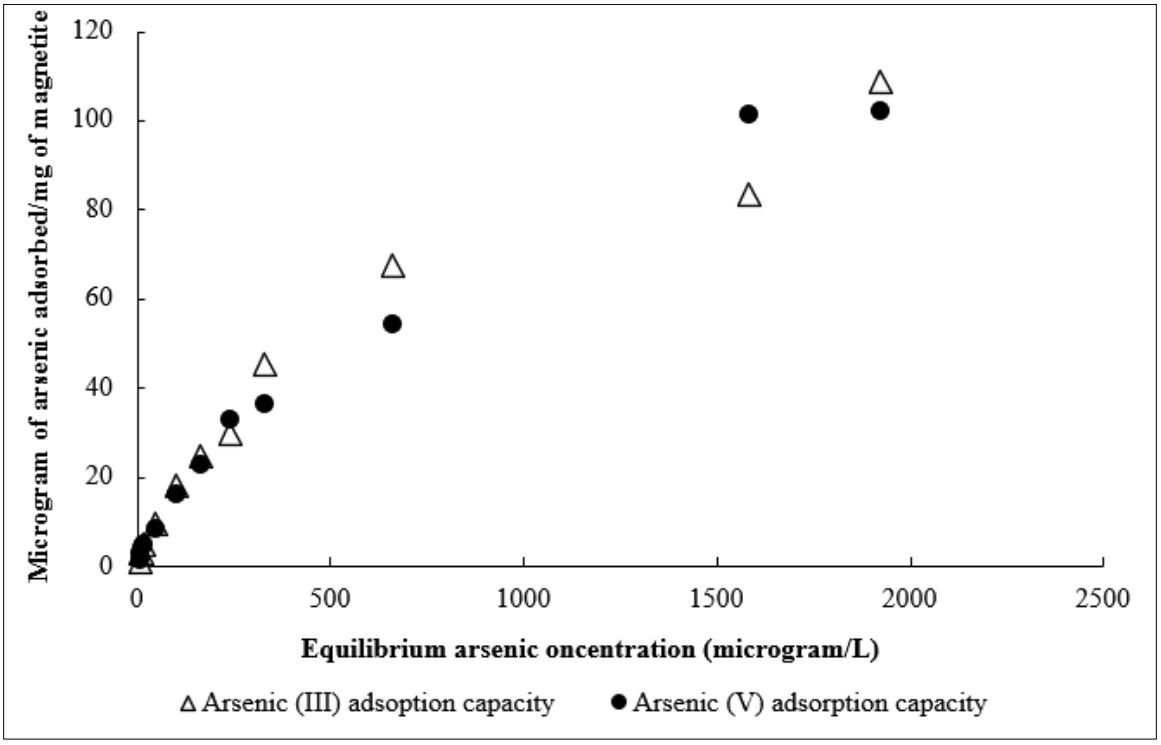

Figure 4: Adsorption of As (III) and As (V) on magnetite at pH 7.0

The adsorption isotherm data were analyzed using Langmuir and Freundlich adsorption isotherm models.

Langmuir equation: $1/q_e = 1/Q_0 + 1/Q_0K_L\ (1/C_e)$

Freundlich equation: $q_e = K_F C_e^{1/n}$

Where Q_0 is the maximum adsorption capacity, q_e is the amount of adsorbed arsenic, C_e is the equilibrium arsenic concentration, K_F and n are the Freundlich constants, and K_L is the Langmuir constant. The Langmuir and Freundlich parameters were obtained from the experimental results given in *Table 2*. The arsenic (V) adsorption on magnetite follows both Freundlich and Langmuir isotherms; though it is better fitting to Freundlich than Langmuir isotherm for arsenic (III) as the coefficient of correlation (R^2) was more reliable for the Freundlich than for the Langmuir model. As (III) and As (V) can follow different isotherm models during adsorption, due to their different oxidation states, charge characteristics, and interaction mechanisms with adsorbents. They may interact differently with the same adsorbent, while both can follow pseudo-second-order kinetics.

Table 2: Langmuir and Freundlich isotherm parameters for adsorption of arsenic

Arsenic Species (pH 7.0)	Langmuir Isotherm			Freundlich Isotherm		
	Q_0	K_L	R^2	K_F	n	R^2
As (III)	125	0.0015	0.85	2.095	1.34	0.96
As (V)	107.5	0.0012	0.97	3.85	1.18	0.97

From Freundlich isotherm parameters, the adsorption intensity parameters (1/n) for As (III) and As (V) are 0.75 and 0.85, indicating a spontaneous and favorable adsorption ($0 < 1/n < 1$) of arsenic on magnetite; values closer to 1 suggest stronger adsorption (Tseng and Wu 2008). The essential characteristics of the Langmuir isotherm can be expressed in terms of a dimensionless constant separation factor, R_L, which is defined as $R_L = 1 / (1+ K_L* C_0)$, where C_0 is the initial arsenic

concentration. In the studied initial arsenic concentrations (10 to 2500 µg /L), the R_L values of As (III) and As (V) indicate that the adsorption of arsenic on magnetite is under favorable conditions ($0< R_L <1$). The decrease in R_L associated with an increase in initial arsenic concentration indicates that the adsorption is more favorable at higher concentrations (Alouiz *et al*. 2024).

3.5. Factors Affecting As (III) Adsorption

3.5.1. Effect of pH

The effect of pH on arsenic (III) adsorption by magnetite was studied in the pH range of 6-8. The effects of pH on arsenic (III) adsorption isotherm are shown in *Figure 5*. Arsenic (III) adsorption isotherms are largely comparable at pH 6 and 7 whereas arsenic (III) removal slightly decreased at pH 8. At pH 6 and 7, As (III) exists mostly as a neutral species (H_3AsO_3) while at pH 8, As (III) begins to exist as negatively charged $H_2AsO_3^-$ species. The neutral species of arsenic (III) forms strong chemical bonds with the magnetite surface at pH 6 and 7 primarily through the formation of strong inner-sphere complexes (Jain R. 2022, Wang *et al*. 2022).

The point of zero charge (pHpzc) for magnetite is typically found around pH 6.8. As solution pH increases beyond the point of zero charge, the surfaces of magnetite particles become increasingly negatively charged due to deprotonation of surface hydroxyl groups. At pH 8, a significant portion of the neutral H_3AsO_3 begins to deprotonate, forming the negatively charged ion, $H_2AsO_3^-$. The resulting electrostatic repulsion between the negatively charged magnetite surface and the newly formed negatively charged As (III) species might be responsible for the slight reduction of As (III) adsorption on the magnetite surface (Thongmueang *et al*. 2024; Wojciechowska and Lendzion-Bielun 2020).

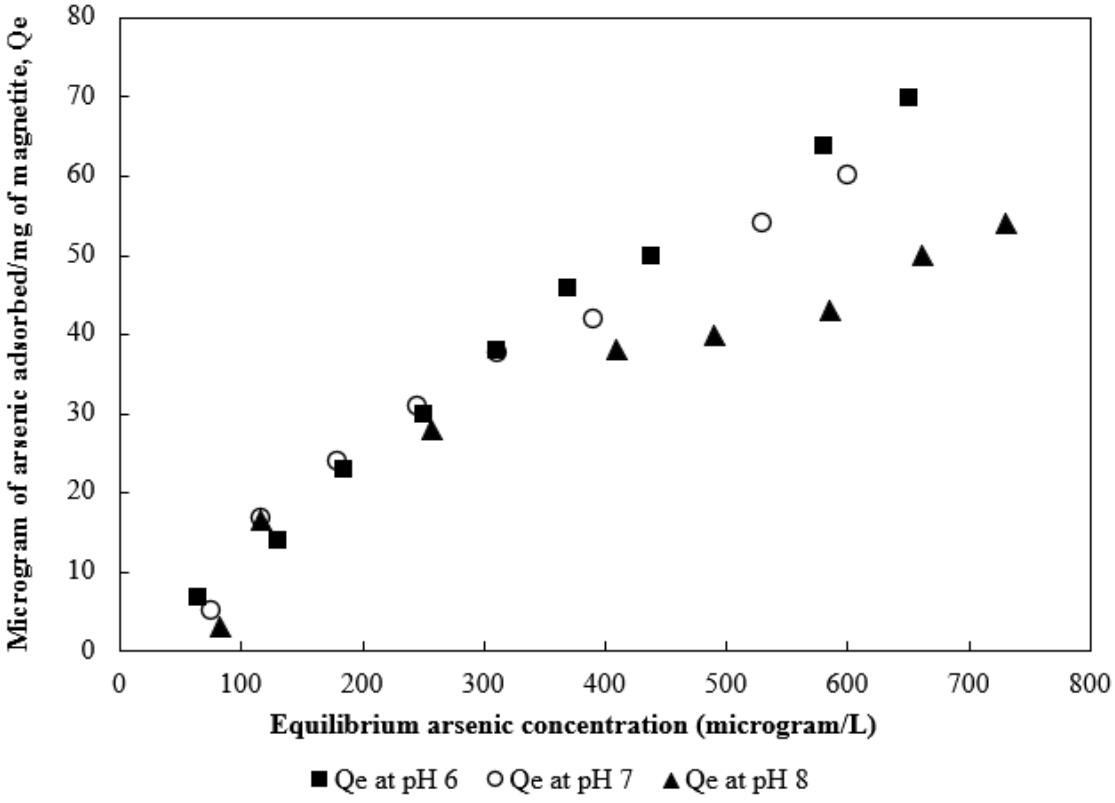

Figure 5: Effects of pH on arsenic (III) adsorption by magnetite

3.5.2. Effect of adsorbent dose

The effect of magnetite dose on arsenic (III) removal at an initial arsenic concentration of 2 mg/L is shown in *Figure 6*. It was observed that the arsenic removal rate increased from 31% to 76% with increasing adsorbent dose, while the adsorption capacity decreased to 62 mg/g from 150 mg/g by increasing the magnetite dose from 4 to 24 mg. The increase in the % removal of arsenic (III) is attributed to the fact that with the increase in adsorbent dose, more active adsorption sites are available for the arsenic (III) to bind. The decrease in estimated adsorption capacity with increased magnetite dose at an arsenic concentration of 2 mg/L was primarily because many active sites remain unsaturated at higher magnetite doses when the initial arsenic concentration is fixed (Yin *et al*. 2021; Das *et al*. 2013).

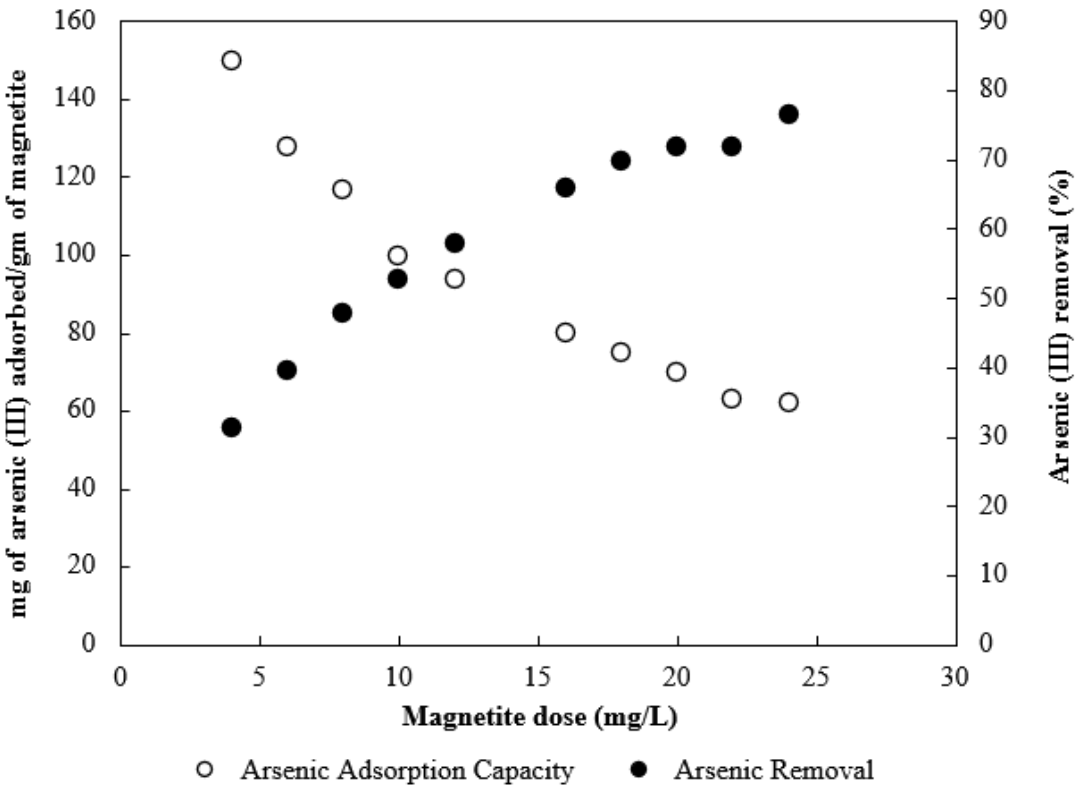

Figure 6: Effects of adsorbent dose on arsenic (III) removal

3.5.3. Effect of initial arsenic concentration

The behavior of As (III) removal was examined at initial arsenic concentrations ranging from 10 to 2500 µg/L. The effect of initial concentration on As (III) removal is shown in *Figure 7*. The result show that the removal efficiency is higher (72-52%) at lower initial arsenic concentration (<100 µg/L). A gradual decrease from 52% to 33% in As (III) removal is observed with increasing the initial arsenic concentrations from 100 to 1000 µg/L. A further decrease in As (III) removal (21%) is observed as initial arsenic concentration increased to 2500 µg/L. The decrease in % removal of arsenic at increased initial concentrations is due to less availability of active sites on the adsorbent surface for further adsorption of arsenic from water. However, increasing initial

arsenic concentration leads to an increase in the arsenic adsorption capacity of magnetite. The arsenic adsorption capacity of magnetite increases from 1.5 to 109 µg/mg with an increase in initial arsenic concentrations from 10 to 2500 µg/L. Increase in the initial arsenic concentration allows the adsorbent to bind more arsenic per unit mass, thus increasing the equilibrium adsorption capacity.

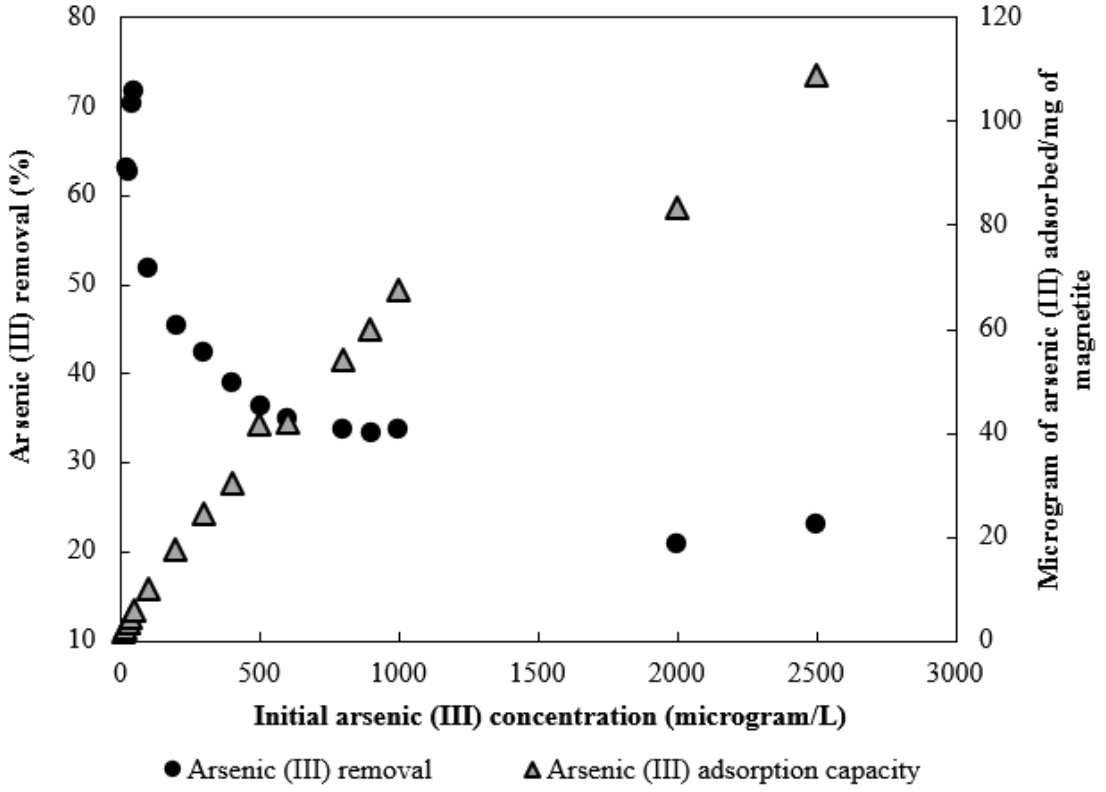

Figure 7: Effects of initial arsenic concentration on arsenic (III) removal

3.6. Comparison and Real-life Application Assessment of Magnetite for As Removal

To compare the arsenic removal efficiency, an adsorption experiment was conducted with magnetite and activated alumina. *Figure 8* compares the arsenic (III) adsorption isotherms of magnetite and activated alumina at pH 7.0. The results show that magnetite is more effective than

activated alumina for arsenic (III) removal. Magnetite exhibits a higher adsorption capacity and faster kinetics for Arsenic (III) removal compared to activated alumina. For magnetite, most of the adsorption reactions reach equilibrium within the first few minutes, whereas for activated alumina it takes more than an hour. The arsenic (III) adsorption capacity of magnetite is significantly higher than activated alumina.

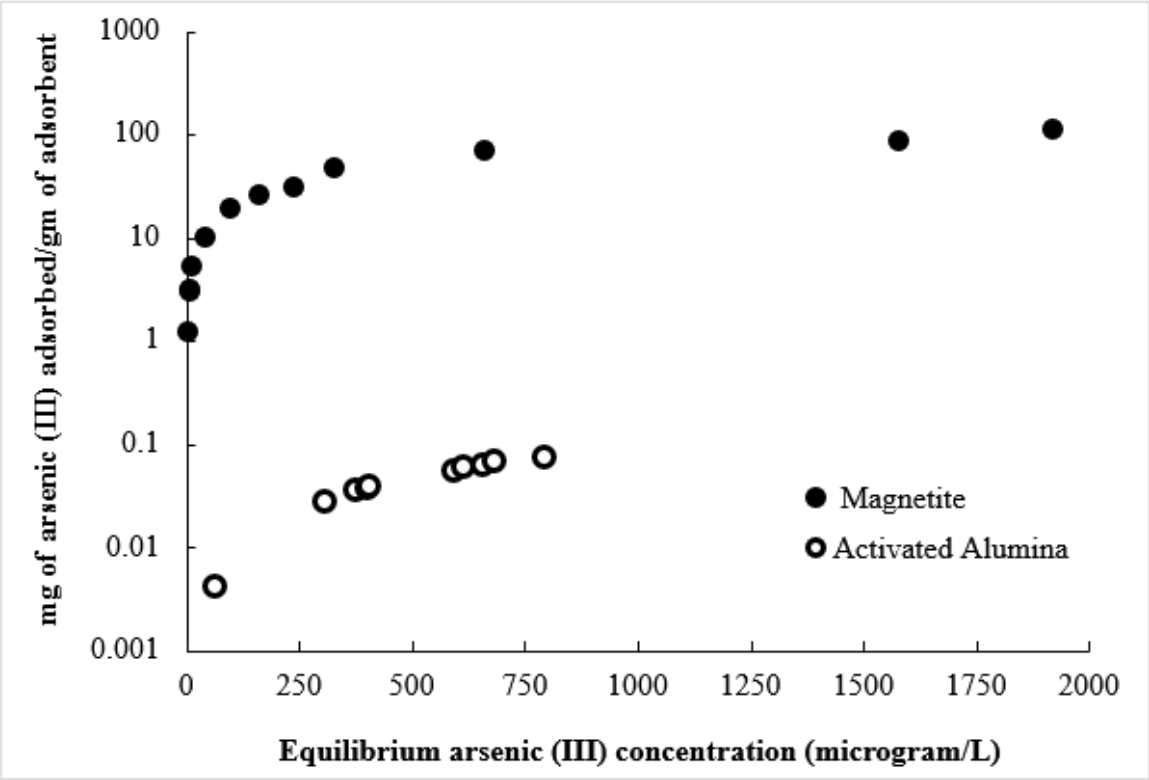

Figure 8: Arsenic (III) removal efficiency of magnetite and activated alumina

To assess the real-life application of magnetite to remove arsenic from contaminated water, an adsorption experiment was conducted using a natural groundwater sample. The groundwater sample was collected from a highly contaminated area of Malda, one of the most severely arsenic affected districts of West Bengal, India. The groundwater sample was thoroughly mixed with 7 mg/L of magnetite at room temperature for 1 hour at a speed of 30-35 rpm. After the adsorption

experiment, the groundwater sample was analyzed for residual arsenic concentration. The result of the preliminary assessment on the arsenic removal capacity of magnetite from a real-life groundwater sample is shown in *Table 3*.

Table 3: Arsenic removal capacity of magnetite from contaminated groundwater sample

Arsenic concentration in groundwater (mg/L)	Residual arsenic concentration in groundwater (mg/L)	Arsenic removal (%)	Arsenic adsorption capacity of magnetite from groundwater (mg/gm)
0.625	0.125	80	71.4

4. Proposed Configuration for a Suspended Adsorbent Filter to Remove Arsenic

Arsenic contamination of drinking water has emerged as one of the global issues across the world. Arsenic removal from water has been proposed and accomplished using a variety of approaches. Groundwater arsenic contamination is a major public health crisis in South and Southeast Asia, especially in Bangladesh and West Bengal, India being the worst-affected regions globally. The majority of the population in this region depends on tube wells for water supply. Thus, cost-effective technologies that are readily available at the household or community level are needed to solve this crisis. Decentralized water treatment for arsenic removal, such as a household filtration unit or community filtration unit is more suitable solution to manage the crisis effectively. Adsorption is regarded as the most economically advantageous method for removing arsenic from water for small scale use because of its high removal efficiency, ease of operation, and cost-effectiveness (Neisan *et al*. 2023; Nicomel *et al*. 2016).

The proposed suspended adsorbent filter could be an appropriate approach for household or community-level arsenic removal system shown in Figure 9. The filter comprises a hollow iron cylinder and a mixer; very loosely packed with magnetite particles to remove arsenic from water through adsorption. The iron cylinder is wrapped with a conductive wire to introduce current from

an external electrical source. Passing an electric current through the wire coiled around the cylinder transforms it into a temporary magnet, commonly known as an electromagnet.

For treatment, arsenic-containing water is poured into the filter with vigorous mixing for about 5-10 minutes, which leads to a surface complexation reaction and arsenic is rapidly absorbed onto the surface of the magnetite particles. The mixing secures and optimizes the surface complexation reaction. Then, the current is passed through the wire which creates a strong, temporary magnetic field within the iron cylinder or filter. This temporary magnetic field causes magnetic separation of the arsenic-loaded magnetite particles, and the particles are removed from the treated water by becoming attracted toward the magnetic source or the surface of the ferromagnetic iron cylinder. Arsenic-free treated water can be collected at this point from the filter outlet. The magnetic field only exists when the electric current flows. The magnetic field within the filter can turn on and off by completing or interrupting the circuit, respectively. Thus, arsenic-contaminated water can be effectively treated by magnetite and separated from magnetite particles for safe consumption using this suspended adsorbent filter. The desired strength of magnetic field that is needed for successful separation of the magnetite particles from treated water can be achieved by optimizing the amount of current flowing through the wire and the number of wire loops or turns around the iron cylinder. Use of the proposed suspended adsorbent filter as decentralized water treatment at household or community level for arsenic removal could be a promising choice to achieve the United Nation's sustainable development goals, since decentralized systems have the potential to manage water resources in a more economical and sustainable way (Pramanik S. 2025).

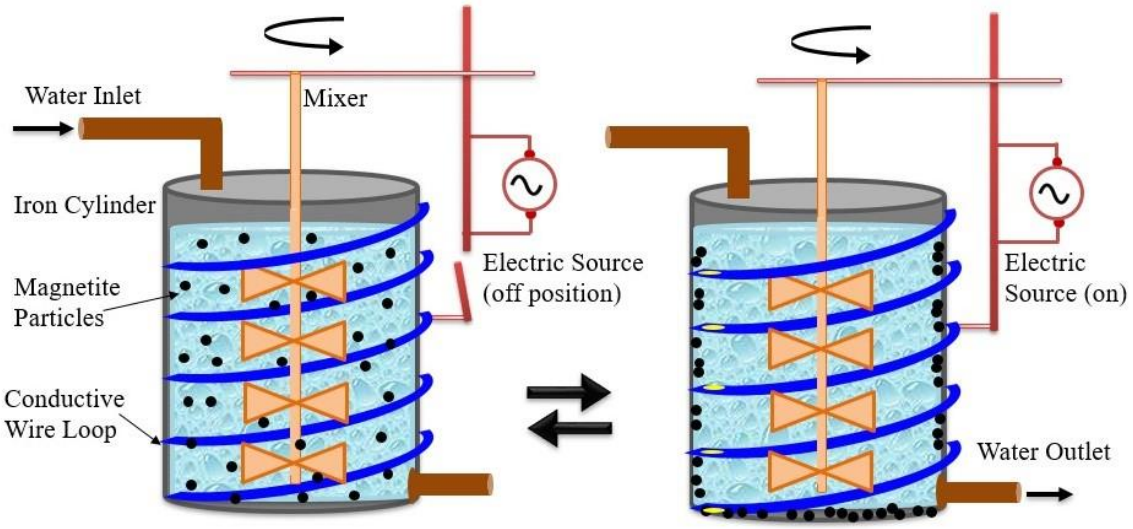

Figure 9: Proposed suspended adsorbent filter for arsenic removal

5. Conclusions

In this study, an electrochemical method has been developed on a laboratory scale to synthesize magnetite and its application to remove arsenic from water. The findings of this research show that magnetite is an efficient material for arsenic removal from water and can be used in a suspended adsorbent filter for water treatment. Magnetite exhibits a higher adsorption capacity and faster kinetics for arsenic removal. It shows a favorable adsorption of arsenic from real-life arsenic-contaminated groundwater. The arsenic adsorption capacity of magnetite is significantly higher than commonly used activated alumina. The proposed suspended adsorbent filter can be a sustainable and affordable solution for household or community level arsenic removal, offering a combination of high-efficiency, rapid kinetics, and easy solid-liquid separation.

Arsenic adsorption and retention capacity of magnetite depend on the size of the particles. The effect of synthesis parameters such as initial pH, electrolyte concentration, voltage, current density, and inter electrode gap on the particle size of magnetite and optimization of the proposed suspended adsorbent filter for real-life application need to be examined in detail and recommended

for future study. The proposed filtration unit could be a viable arsenic and fluoride removal technology to manage the dependency on groundwater effectively to achieve the United Nation's sustainable Development Goals (SDGs).

Acknowledgments

The article is part of the author's master's research project. The author thankfully acknowledges Professor Sanjeev Chaudhari for supervising the project at CESE, Indian Institute of Technology Bombay, India.

References

Alouiz I., Benhadj M., Dahmane E., Mouadili A., Sennoune M., Amarouch M. Y., Mazouzi D. (2024). Exploring the potential of olive pomace derived activated charcoal as an efficient adsorbent for methylene blue dye: a comprehensive investigation of isotherms, kinetics, and thermodynamics. *Materials Research Express*, 11, 055504.

Bundschuh J., Niazi N. K., Alam M. A., Berg M., Herath I., Tomaszewska B., Maity J. P., Ok Y. S. (2022). Global arsenic dilemma and sustainability. *Journal of Hazardous Materials,* 436, 129197.

Cabrera L., Gutierrez S., Menendezb N., Morales M. P., Herrasti P. (2008). Magnetite nanoparticles: electrochemical synthesis and characterization. *Electrochimica Acta*, 53, 3436–3441.

Chaki S. H., Malek T. J., Chaudhary M. D., Tailor J. P., Deshpande M. P. (2015). Magnetite Fe3O4 nanoparticles synthesis by wet chemical reduction and their characterization. *Advances in Natural Sciences: Nanoscience and Nanotechnology*, 6, 035009.

Chakraborti D., Singh S. K., Rahman M. M., Dutta R. N., Mukherjee S. C., Pati S., Kar P. B. (2018). Groundwater arsenic contamination in the Ganga river basin: a future health danger. *International Journal of Environmental Research and Public Health,* 15, 180.

Cheng W., Tang K., Qi Y., Sheng J., Liu Z. (2010). One-step synthesis of superparamagnetic monodisperse porous Fe_3O_4 hollow and core-shell spheres. *Journal of Materials Chemistry,* 20, 1799-1805.

Clifford D. A., Ghurye G., Tripp A. R. (1999). Development of an anion exchange process for arsenic removal from water. Arsenic Exposure and Health Effects III, Proceedings of the Third International Conference on Arsenic Exposure and Health Effects. 379-387.

Das B., Devi R. R., Umlong I. M., Borah K., Banerjee S., Talukdar A. K. (2013). Arsenic (III) adsorption on iron acetate coated activated alumina: thermodynamic, kinetics and equilibrium approach. *Journal of Environmental Health Sciences and Engineering*, 11 (42).

Fajaroh F., Setyawan H., Widiyastuti W., Winardi S. (2012). Synthesis of magnetite nanoparticles by surfactant-free electrochemical method in an aqueous system. *Advanced Powder Technology*, 23, 328–333.

Farrell J. W., Fortner J., Work S., Avendano C., Gonzalez-Pech N. I., Araiza R. Z., Li Q., Alvarez P. J. J., Colvin V., Kan A., Tomson M. (2014). Arsenic removal by nanoscale magnetite in Guanajuato, Mexico. *Environmental Engineering Science*, 31(7).

Feng L., Cao M., Ma X., Zhu Y., Hu C. (2012). Superparamagnetic high-surface-area Fe_3O_4 nanoparticles as adsorbents for arsenic removal. *Journal of Hazardous Materials*, 217-218, 439-446.

Foster S. A., Pennino M. J., Compton J. E., Leibowitz S. G., Kile M. L. (2019). Arsenic drinking water violations decreased across the United States following revision of the maximum contaminant level. *Environmental Science and Technology*, 53(19), 11478–11485.

Franger S., Berthet P., Berthon J. (2004). Electrochemical synthesis of Fe_3O_4 nanoparticles in alkaline aqueous solutions containing complexing agents. *Journal of Solid State Electrochemistry*, 8, 218–223.

Hering J. G., Chen P. U., Wilkie J. A., Elimelech M. (1997). Arsenic removal from drinking water during coagulation. *Journal of Environmental Engineering*, 123 (8), 800-807.

Ho Y. S. and McKay G. (1999). Pseudo-second order model for sorption processes. *Process Biochemistry*, 34, (5), 451-465.

Jain R. (2022). Recent advances of magnetite nanomaterials to remove arsenic from water. *Royal Society of Chemistry Advances*, 12, 32197–32209.

Johnson D.L. and Pilson M.E.Q. (1972). Spectrophotometric determination of arsenite; arsenate and phosphate in natural waters, *Analytica Chimica Acta*, 58, 289 – 299.

Johnston R. B. (2016). Arsenic and the 2030 agenda for sustainable development. Arsenic Research and Global Sustainability—Proceedings of the 6th International Congress on Arsenic in the Environment, pp.12-14, Routledge.

Kanel S. R., Manning B., Charlet L., Choi H. (2005). Removal of As (III) from groundwater by nanoscale zero-valent iron. *Environmental Science and Technology*, 39, 1291-1298.

Manning B. A., Hunt M. L., Amrhein C. and Yarmoff J. A. (2002). Arsenic (III) and arsenic (V) reaction with zerovalent iron corrosion products. *Environmental Science and Technology*, 36, 5455-5461.

Marghade D., Mehta G., Shelare S., Jadhav G., Nikam K. C. (2023). Arsenic contamination in Indian groundwater: from origin to mitigation approaches for a sustainable future. *Water*, 15, 4125.

McGavisk E., Roberson J. A., Seidel C. (2013). Using community economics to compare arsenic compliance and noncompliance. *Journal of Americal Water Works Association*, 105 (3), E115 - E126.

Mohan D. and Pittman C. U. (2007). Arsenic removal from water/wastewater using adsorbents – a critical review. *Journal of Hazardous Materials*, 142, 1-53.

Neisan R. S., Cata Saady N. M., Bazan C., Zendehboudi S., Al-nayili A., Abbassi B., Chatterjee P. (2023). Arsenic removal by adsorbents from water for small communities' decentralized systems: performance, characterization, and effective parameters. *Clean Technologies*, 5, 352–402.

Nicomel N. R., Leus K., Folens K., Van Der Voort P., Laing G. D. (2016). Technologies for arsenic removal from water: current status and future perspectives. *International Journal of Environmental Research and Public Health*, 13(1), 62.

Nikic J., Tubic A.,Watson M., Maletic S., Šolic M., Majkic T., Agbaba J. (2019). Arsenic removal from water by green synthesized magnetic nanoparticles. *Water*, 11, 2520.

Pramanik S. (2025). Introduction of a nature-based sustainable technology to mitigate climate change-driven water pollution in rivers and lakes. [Preprint]. EarthArXiv. https://doi.org/10.31223/X5SM7D

Qasem N. A. A., Mohammed R. H., Lawal D. U. (2021). Removal of heavy metal ions from wastewater: a comprehensive and critical review. *Npj Clean Water*, 36.

Reséndiz-Ramírez R., Rodríguez-López A., Díaz-Real J. A., Delgado-Arenas H. F., Osornio-Villa A., Hernández-Leos R., Vivier V., Antaño-López R. (2022). Reaction mechanisms of the electrosynthesis of magnetite nanoparticles studied by electrochemical impedance spectroscopy. *ACS Omega*, 7, 761−772.

Sarker M. M. R., Ahmad M. M., Deb U. (2023). Arsenic and arsenicosis threat to achieve the sustainable development goals. Arsenic in the Environment: Bridging Science to Practice for Sustainable Development – van der Wal, Ahmad, Petrusevski, Weijma, Savic, van der Wens, Beerendonk, Bhattacharya, Bundschuh & Naidu (Eds), ISBN 978-1-032-32928-4.

Shaji E., Santosh M., Sarath K. V., Prakash P., Deepchand V., Divya B. V. (2021). Arsenic contamination of groundwater: a global synopsis with focus on the Indian peninsula. *Geoscience Frontiers*, 12, 101079.

Smith A. H., Lingas E. O., Rahman M. (2000). Contamination of drinking-water by arsenic in Bangladesh: a public health emergency. *Bulletin of the World Health Organization*, 78 (9), 1093-1103.

Starowicz M., Starowicz P., Zukrowski J., Przewoznik J., Lemanski A., Kapusta C., Banas J. (2011). Electrochemical synthesis of magnetic iron oxide nanoparticles with controlled size. *Journal* of *Nanoparticle Research*, 13, 7167–7176.

Thongmueang K., Boonkaewwan S., Chotpantarat S. (2024). Effect of pH on arsenite (As^{3+}) sorption on goethite: Kinetic and equilibrium experiments. *Case Studies in Chemical and Environmental Engineering*, 9, 100598.

Tseng R. L. and Wu F. C. (2008). Inferring the favorable adsorption level and the concurrent multi-stage process with the Freundlich constant. *Journal of Hazardous Materials*, 155, 277-287.

Wang C., Liu X., Chen P., Li K. (2015). Superior removal of arsenic from water with zirconium metalorganic framework UiO-66. *Scientific Reports*, 5, 16613.

Wang Y., Zhang L., Guo C., Gao Y., Pan S., Liu Y., Li X., Wang Y. (2022). Arsenic removal performance and mechanism from water on iron hydroxide nanopetalines. *Scientific Reports*, 12, 17264.

Wojciechowska A. and Lendzion-Bielun Z. (2020). Synthesis and characterization of magnetic nanomaterials with adsorptive properties of arsenic ions. *Molecules*, 25, 4117.

Yadav A. K., Yadav H. K., Naz A., Koul M., Chowdhury A., Shekhar S. (2022). Arsenic removal technologies for middle- and low-income countries to achieve the SDG-3 and SDG-6 targets: A review. *Environmental Advances*, 9, 100262.

Yin Y., Xu G., Li L., Qiao C., Xiao Y., Ma T., Liu C. (2021). Removal of inorganic arsenic from aqueous solution by Fe-modified ceramsite: batch studies and remediation trials. *Water Science and Technology*, 83 (7), 1522-1534.

Zhang Y. J., Lin Y. W., Chang C. C., Wu T. M. (2010). Magnetic properties of hydrophilic iron oxide/polyaniline nanocomposites synthesized by in situ chemical oxidative polymerization. *Synthetic Metals*, 160, 1086–1091.